

AGN-driven convection in galaxy-cluster plasmas

Benjamin D. G. Chandran

benjamin-chandran@uiowa.edu

Department of Physics & Astronomy, University of Iowa

ABSTRACT

This paper describes how active galactic nuclei can heat galaxy-cluster plasmas by driving convection in the intracluster medium. A model is proposed in which a central supermassive black hole accretes intracluster plasma at the Bondi rate \dot{M}_{Bondi} and powers a radio source. The central radio source produces cosmic rays, which mix into the thermal plasma. The cosmic-ray luminosity L_{cr} is $\propto \dot{M}_{\text{Bondi}} c^2$. The cosmic-ray pressure gradient drives convection, which causes plasma heating. It is assumed that plasma heating balances radiative cooling. The plasma heating rate is self-regulating because \dot{M}_{Bondi} is a decreasing function of the specific entropy near the cluster center s_0 ; if heating exceeds cooling, then s_0 increases, \dot{M}_{Bondi} and L_{cr} decrease, and the convective heating rate is reduced. This paper focuses on the role of intracluster magnetic fields, which affect convection by causing heat and cosmic rays to diffuse primarily along magnetic field lines. A new stability criterion is derived for convection in a thermal-plasma/cosmic-ray fluid, and equations for the average fluid properties in a convective cluster are obtained with the use of a nonlocal two-fluid mixing length theory. Numerical solutions of the model equations compare reasonably well with observations without requiring fine tuning of the model parameters.

Subject headings: cooling flows — galaxies:clusters:general — galaxies:active — convection — magnetic fields — turbulence

1. Introduction

In many clusters of galaxies the radiative cooling time of intracluster plasma within the central 50 kpc is shorter than a cluster's age. In the cooling-flow model plasma heating is neglected and the rate at which plasma cools to low temperatures (\dot{M}_{CF}) is large, exceeding $10^3 M_{\odot} \text{yr}^{-1}$ in some clusters (Fabian 1994). Recent high-spectral-resolution x-ray

observations, however, show that the actual rate at which plasma cools to low temperatures is $\lesssim 0.1\dot{M}_{\text{CF}}$ (Peterson et al 2001, 2003; Böhringer et al 2001; Tamura et al 2001; Molendi & Pizzolato 2001). This discrepancy, some times referred to as the “cooling-flow problem,” suggests that plasma heating approximately balances radiative cooling in cluster cores. Plasma heating is also relevant to other unsolved problems in the study of galaxy clusters. Numerical simulations of cluster formation show that some heat source in addition to supernovae is needed to explain observed temperature and density profiles, star-formation histories, and mass-temperature and luminosity-temperature scaling relations (Suginohara & Ostriker 1998; Lewis et al 2000; Voit et al 2002; Tornatore et al 2003; Nagai & Kravtsov 2004; Borgani et al 2004; Dolag et al 2004).

This paper focuses on plasma heating by active galactic nuclei (AGN) at the centers of clusters. The importance of AGN heating is suggested by the observation that almost all clusters with strongly cooling cores possess active central radio sources (Eilek 2004). Several mechanisms have been considered for transferring AGN power to intracluster plasma, including magnetohydrodynamic (MHD) wave-mediated plasma heating by cosmic rays (Böhringer & Morfill 1988; Rosner & Tucker 1989; Loewenstein, Zweibel, & Begelman 1991), Compton heating (Binney & Tabor 1995; Ciotti & Ostriker 1997, 2001; Ciotti, Ostriker, & Pellegrini 2004), shocks (Tabor & Binney 1993, Binney & Tabor 1995), and cosmic-ray bubbles produced by the central AGN (Churazov et al 2001, 2002; Reynolds 2002; Brüggén 2003; Reynolds et al 2005). Such bubbles can heat intracluster plasma by generating turbulence (Loewenstein & Fabian 1990, Churazov et al 2004) and sound waves (Fabian et al 2003; Ruszkowski, Brüggén, & Begelman 2004a,b) and by doing pdV work (Begelman 2001, 2002; Ruszkowski & Begelman 2002; Hoeft & Brüggén 2004). Although considerable progress has been made, the coupling between AGN and cluster plasmas is still not well understood.

The present paper describes how AGN can heat intracluster plasmas by driving convection. In section 2 physical arguments are used to obtain the convective stability criterion in magnetized low-density plasmas containing cosmic rays. Section 3 develops a steady-state model of convective intracluster plasmas. In this model, a central supermassive black hole accretes intracluster plasma at the Bondi rate \dot{M}_{Bondi} , leading to cosmic-ray production by a central radio source. The cosmic-ray luminosity L_{cr} is taken to be proportional to $\dot{M}_{\text{Bondi}}c^2$, and it is assumed that the cosmic-rays mix into the thermal intracluster plasma. The cosmic-ray pressure gradient drives convection, which is treated with a two-fluid (thermal-plasma and cosmic-ray) mixing length theory. Convection heats the plasma in three ways, by mixing hot plasma from the outer regions of a cluster in towards the center of the cluster, by providing a vehicle for cosmic-ray pressure to do work on the thermal plasma, and through the viscous dissipation of turbulent motions. It is assumed that plasma heating balances radiative cooling. The heating rate is self-regulating because \dot{M}_{Bondi} is a decreasing func-

tion of the specific entropy near the center of the cluster, s_0 ; if heating exceeds cooling, then s_0 rises, \dot{M}_{Bondi} falls, and the convective heating rate drops (Nulsen 2004; Böhringer 2004a). The model leads to a set of coupled ordinary differential equations that are solved numerically using a shooting method.

In section 4 the model is compared to observations. For a single choice of the model’s free parameters, the solutions to the model equations compare reasonably well with observations of the Virgo cluster, the Perseus cluster, and Abell 478. However, the model underestimates the plasma density in the central ~ 30 kpc. This discrepancy may arise because the model does not properly account for the observed incomplete mixing of cosmic rays into the thermal plasma in the central region, a point discussed further in section 4.

The model differs from an earlier two-fluid convection model (Chandran 2004—hereafter paper I) primarily by including the effects of anisotropic conduction and cosmic-ray diffusion on convection. Anisotropic transport allows smaller cosmic-ray pressures to drive convection, which enables the model of the present paper to provide a better fit to the data. (In paper I, a larger central cosmic-ray pressure leads to an even smaller thermal pressure and density in the central ~ 30 kpc.)

In addition to the topics mentioned above, section 4 also describes the relation of the model to other turbulent heating models and addresses the consequences of the model for diffuse gamma-ray emission from clusters and the mixing of heavy elements in the intracluster medium.

2. Convective stability in a low-density plasma containing cosmic rays and a weak magnetic field

In this section, physical arguments are used to obtain the stability criterion for convection in a magnetized plasma/cosmic-ray fluid. Figure 1 depicts a fluid parcel rising from an initial radial coordinate r_0 to a final coordinate $r_1 = r_0 + \Delta r$. Only instabilities on length scales $\ll r_0$ are considered. The gravitational acceleration \mathbf{g} is in the $-\hat{\mathbf{r}}$ direction. The horizontal solid line is a field line in the equilibrium magnetic field, which is taken to be perpendicular to \mathbf{g} . The dashed line depicts how the field line is displaced as the fluid parcel rises. It is assumed that the magnetic field is strong enough so that heat and cosmic rays diffuse primarily along magnetic field lines (a requirement easily met in clusters) but sufficiently weak that the Lorentz force can be ignored. The latter assumption may be too restrictive for clusters, but is maintained throughout this paper for simplicity. It is assumed that equilibrium quantities depend only on r . The equilibrium temperature,

thermal-particle density, and cosmic ray pressure at r_0 and r_1 are denoted $(T_0, n_0, p_{\text{cr},0})$ and $(T_1, n_1, p_{\text{cr},1})$, respectively. Initially, the fluid properties in the parcel equal the equilibrium values at r_0 . After the parcel is displaced to r_1 , the fluid properties within the parcel are denoted $(T_f, n_f, p_{\text{cr},f})$. Requiring that the total pressure within the displaced parcel equal the total pressure in the surrounding medium gives

$$n_f k_B T_f + p_{\text{cr},f} = n_1 k_B T_1 + p_{\text{cr},1}. \quad (1)$$

If the frequency ω of the fluid's linear modes were constrained to be either real or imaginary, then near marginal stability ω would approach 0 and the time scale for the parcel's displacement to grow or oscillate would be very long. In this case there would be plenty of time for thermal conduction and cosmic-ray diffusion to smooth out T and p_{cr} along the displaced magnetic field lines, giving $T_f = T_0$ and $p_{\text{cr},f} = p_{\text{cr},0}$. Thus, if ω^2 were constrained to be real, then near marginal stability equation (1) could be rewritten

$$n_f k_B T_0 + p_{\text{cr},0} = n_1 k_B \left(T_0 + \Delta r \frac{dT}{dr} \right) + p_{\text{cr},0} + \Delta r \frac{dp_{\text{cr}}}{dr}, \quad (2)$$

where T_1 and $p_{\text{cr},1}$ have been expanded in a Taylor series about $r = r_0$, and terms that are quadratic or higher order in Δr have been discarded. Equivalently,

$$(n_f - n_1) k_B T_0 = \Delta r \left(n_1 k_B \frac{dT}{dr} + \frac{dp_{\text{cr}}}{dr} \right). \quad (3)$$

If $n_f - n_1 > 0$, the displaced parcel is heavier than its surroundings and sinks back down, and the fluid is stable to convection. Conversely, if $n_f - n_1 < 0$, the parcel is buoyant and the fluid is unstable. (It is assumed that the mean molecular weight is a constant.) Thus, if ω^2 were real, the convective stability criterion would be

$$n k_B \frac{dT}{dr} + \frac{dp_{\text{cr}}}{dr} > 0. \quad (4)$$

[The subscripts can be dropped in equation (4) since Δr is taken to be small.] In a future publication a linear stability analysis will be used to show that equation (4) is in fact the necessary and sufficient condition for convective stability in the plasma/cosmic-ray fluid, even though ω^2 is not in general real.¹ In the absence of cosmic rays, equation (4) reduces to the stability criterion $dT/dr > 0$ derived by Balbus (2001). [In stellar interiors, heat is transported primarily by photons, the conductivity is isotropic, and Balbus's criterion does not apply (Balbus 2001).]

¹Equation (4) is the $\gamma \rightarrow 1$ and $\gamma_{\text{cr}} \rightarrow 0$ limit of equation (28) of paper I, essentially because T and p_{cr} can be treated as constant in the displaced parcel near marginal stability.

In section 3, the above physical arguments are extended in an approximate way to galaxy clusters, in which the magnetic field lines are tangled. The same stability criterion is recovered, essentially because conduction and diffusion still act to resist changes in the temperature and cosmic-ray pressure of displaced fluid elements. Throughout most of a cluster, dT/dr is much less than T/r . On the other hand, for cosmic rays diffusing outwards from a central point source, $dp_{\text{cr}}/dr \sim -p_{\text{cr}}/r$. When $dT/dr \ll T/r$ and $dp_{\text{cr}}/dr \sim -p_{\text{cr}}/r$, equation (4) implies that cosmic rays can drive convection even when $p_{\text{cr}} \ll p$. Centrally produced cosmic rays in clusters are thus highly destabilizing to convection.

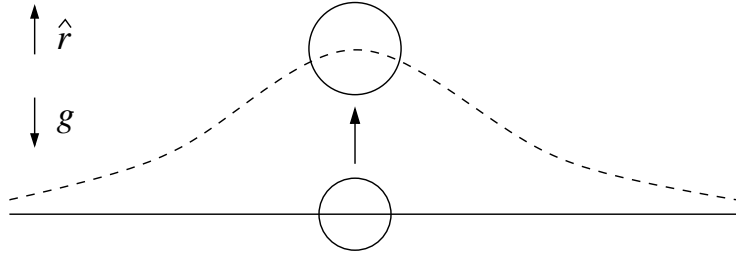


Fig. 1.— A rising fluid parcel and one of the magnetic field lines threading the parcel.

3. The AGN-driven convection model

The intracluster medium is described using a standard set of two-fluid equations for cosmic rays and thermal plasma (Drury & Volk 1981, Jones & Kang 1990), modified to include thermal conduction, viscous dissipation, and radiative cooling:

$$\frac{d\rho}{dt} = -\rho \nabla \cdot \mathbf{v}, \quad (5)$$

$$\rho \frac{d\mathbf{v}}{dt} = -\nabla(p + p_{\text{cr}}) - \rho \nabla \Phi - \nabla \cdot \mathbf{\Pi}, \quad (6)$$

$$\frac{dp}{dt} = -\gamma p \nabla \cdot \mathbf{v} + (\gamma - 1)[H_{\text{diss}} + \nabla \cdot (\kappa \cdot \nabla T) - R], \quad (7)$$

and

$$\frac{dp_{\text{cr}}}{dt} = -\gamma_{\text{cr}} p_{\text{cr}} \nabla \cdot \mathbf{v} + \nabla \cdot (\mathbf{D} \cdot \nabla p_{\text{cr}}) + (\gamma_{\text{cr}} - 1) \dot{E}_{\text{inj}}, \quad (8)$$

where

$$\frac{d}{dt} \equiv \frac{\partial}{\partial t} + \mathbf{v} \cdot \nabla, \quad (9)$$

ρ is the plasma density, \mathbf{v} is the bulk velocity of the two-fluid mixture, p and p_{cr} are the plasma and cosmic-ray pressures, T is the plasma temperature, Φ is the gravitational potential, $\mathbf{\Pi}$ is the viscous stress tensor, γ and γ_{cr} are the plasma and cosmic-ray adiabatic indices (which are treated as constants), H_{diss} is the rate of viscous heating, κ is the thermal conductivity tensor, R is the radiative cooling rate, \dot{E}_{inj} is the rate of injection of cosmic-ray energy per unit volume by the central radio source, and \mathbf{D} is an effective momentum-averaged cosmic-ray diffusion tensor.²

Cluster magnetic fields are easily strong enough to cause cosmic rays and heat to diffuse primarily along field lines, so that

$$\kappa \simeq \kappa_{\parallel} \hat{b}\hat{b}, \quad (10)$$

and

$$\mathbf{D} \simeq D_{\parallel} \hat{b}\hat{b}, \quad (11)$$

where \hat{b} is the magnetic field unit vector, and κ_{\parallel} and D_{\parallel} are the parallel conductivity and diffusivity. Cluster fields may also be strong enough that the Lorentz force and resistive dissipation are important [see, e.g., Pen, Matzner, & Wong (2003)], but for simplicity these terms are neglected in equations (6) and (7). The parallel conductivity is set equal to the Spitzer conductivity for a non-magnetized plasma,

$$\kappa_{\parallel} = \kappa_{\text{S}} = 9.2 \times 10^{30} n_e k_{\text{B}} \left(\frac{k_{\text{B}} T}{5 \text{ keV}} \right)^{5/2} \left(\frac{10^{-2} \text{ cm}^{-3}}{n_e} \right) \left(\frac{37}{\ln \Lambda_{\text{c}}} \right) \frac{\text{cm}^2}{\text{s}}, \quad (12)$$

where n_e is the electron density, k_{B} is the Boltzmann constant, and $\ln \Lambda_{\text{c}}$ is the Coulomb logarithm. The value of D_{\parallel} is discussed below.

The analytic fit of Tozzi & Norman (2001) is used to approximate the full cooling function for free-free and line emission:

$$R = n_i n_e \left[0.0086 \left(\frac{k_{\text{B}} T}{1 \text{ keV}} \right)^{-1.7} + 0.058 \left(\frac{k_{\text{B}} T}{1 \text{ keV}} \right)^{0.5} + 0.063 \right] \cdot 10^{-22} \text{ ergs cm}^3 \text{ s}^{-1}, \quad (13)$$

where n_i is the ion density and the numerical constants correspond to 30% solar metallicity. The mean molecular weight per electron $\mu_e = \rho/n_e m_H$ is set equal to 1.18, and the ratio n_i/n_e

²Equations (7) and (8) are the same as the equations used in paper I, except that \mathbf{D} and κ are taken to be isotropic in paper I, and the definition of \mathbf{D} in paper I corresponds to $(\gamma_{\text{cr}} - 1)^{-1}$ times the value of \mathbf{D} appearing in equation (8).

is set equal to 0.9. Radiative cooling of cosmic rays is ignored, which is reasonable if protons make the dominant contribution to the cosmic-ray pressure. Coulomb interactions between cosmic rays and thermal plasma are also neglected.

The gravitational potential is taken to be the sum of a cluster potential and a central galaxy potential,

$$\Phi = \Phi_c + \Phi_g, \quad (14)$$

with Φ_c corresponding to a fixed NFW dark matter density profile (Navarro, Frenk, & White 1997),

$$\rho_{\text{DM}} = \frac{\delta_c \rho_{\text{crit}} r_s^3}{r(r + r_s)^2}, \quad (15)$$

where

$$\delta_c = \frac{200}{3} \frac{c^3}{[\ln(1+c) - c/(1+c)]}, \quad (16)$$

r_s is the scale radius, c is the concentration parameter, and $\rho_{\text{crit}} = 3H^2/8\pi G$ is the critical density at the redshift of the cluster (calculated assuming $\Omega_0 = 0.3$, $\Omega_{\Lambda,0} = 0.7$, and $H_0 = 70 \text{ km s}^{-1}\text{Mpc}^{-1}$). The central galaxy potential is set equal to

$$\Phi_g = \frac{v_g^2}{2} \ln \left[1 + \left(\frac{r}{r_g} \right)^2 \right], \quad (17)$$

where v_g and r_g are constants, and v_g is the circular velocity for $r \gg r_g$ if Φ_c is ignored.

Since the intracluster medium is turbulent, each fluid quantity is written as an average value plus a turbulent fluctuation:

$$\mathbf{v} = \langle \mathbf{v} \rangle + \delta \mathbf{v}, \quad (18)$$

$$p = \langle p \rangle + \delta p, \quad (19)$$

etc. The averaged quantities are taken to be spherically symmetric and independent of time. Equations (6) through (8) are then averaged. The viscous and inertial terms are neglected in the average of equation (6), so that

$$\frac{d}{dr} \langle p_{\text{tot}} \rangle = -\langle \rho \rangle \frac{d\Phi}{dr}, \quad (20)$$

where

$$p_{\text{tot}} = p + p_{\text{cr}}. \quad (21)$$

The averages of equations (7) and (8) can be written

$$\nabla \cdot \mathbf{F} = -W + \langle H_{\text{diss}} + \nabla \cdot (\kappa \cdot \nabla T) - R \rangle, \quad (22)$$

and

$$\nabla \cdot \mathbf{F}_{\text{cr}} = -W_{\text{cr}} + \frac{\langle \nabla \cdot (\mathbf{D} \cdot \nabla p_{\text{cr}}) \rangle}{\gamma_{\text{cr}} - 1} + \langle \dot{E}_{\text{inj}} \rangle, \quad (23)$$

where

$$\mathbf{F} = F \hat{\mathbf{r}} = \frac{\langle \mathbf{v} p \rangle}{\gamma - 1} \quad (24)$$

is the average internal energy flux,

$$\mathbf{F}_{\text{cr}} = F_{\text{cr}} \hat{\mathbf{r}} = \frac{\langle \mathbf{v} p_{\text{cr}} \rangle}{\gamma_{\text{cr}} - 1}, \quad (25)$$

$$W = \langle p \nabla \cdot \mathbf{v} \rangle, \quad (26)$$

and

$$W_{\text{cr}} = \langle p_{\text{cr}} \nabla \cdot \mathbf{v} \rangle. \quad (27)$$

The fluctuating quantities are treated as small, so $\langle R \rangle$ can be approximately obtained by replacing n_e , n_i , and T in equation (13) by their average values, and to a good approximation

$$\langle p \rangle = \frac{k_B \langle \rho \rangle \langle T \rangle}{\mu m_H}. \quad (28)$$

The mean molecular weight μ is set equal to 0.62.

To obtain an average of the conduction and cosmic-ray diffusion terms, the disordered geometry of the magnetic field must be taken into account. Within the central 100 kpc of a cluster, the characteristic magnetic-field length scale l_B is probably in the range 1 – 10 kpc (Kronberg 1994, Taylor et al 2001, 2002, Vogt & Ensslin 2003, Ensslin & Vogt 2005), which is much smaller than the temperature gradient length scale $L_T = \langle T \rangle / (d\langle T \rangle / dr)$. The field is also probably turbulent, with an inertial range of (shear-Alfvén-like) magnetic fluctuations on scales ranging from $\sim l_B$ down to the proton gyroradius (Goldreich & Sridhar 1995, Quataert 1998, Narayan & Medvedev 2001). The chaotic trajectories of field lines lead to an isotropic effective conductivity κ_T for heat transport over distances $\gg l_B$, with κ_T reduced relative to κ_{\parallel} (Rechester & Rosenbluth 1978, Chandran & Cowley 1998). The degree of reduction is not known with great accuracy, but approximate theoretical studies find that the reduction is by a factor of $\sim 5 - 10$ (Narayan & Medvedev 2001, Chandran & Maron 2004, Maron, Chandran, & Blackman 2004). In this paper, it is assumed that

$$\kappa_T = \theta \kappa_{\parallel}, \quad (29)$$

where the constant θ is a free parameter. The average of the conductive heating term is taken to satisfy the equation

$$\langle \nabla \cdot (\kappa \cdot \nabla T) \rangle = \frac{1}{r^2} \frac{d}{dr} \left[r^2 \kappa_T \frac{d}{dr} \langle T \rangle \right], \quad (30)$$

with T set equal to $\langle T \rangle$ in equation (12). Similarly, it is assumed that

$$\langle \nabla \cdot (\mathbf{D} \cdot \nabla p_{\text{cr}}) \rangle = \frac{1}{r^2} \frac{d}{dr} \left[r^2 D_{\text{cr}} \frac{d}{dr} \langle p_{\text{cr}} \rangle \right]. \quad (31)$$

The value of D_{cr} is taken to be

$$D_{\text{cr}} = \sqrt{D_0^2 + v_d^2 r^2}, \quad (32)$$

where the constants D_0 and v_d are free parameters. The v_d term is loosely motivated by a simplified picture of cosmic-ray “self-confinement,” in which cosmic rays are scattered by waves generated by the streaming of cosmic rays along field lines. If, contrary to fact, the field lines were purely radial, efficient self-confinement would limit the average radial velocity of the cosmic rays to the Alfvén speed v_A , allowing the cosmic rays to travel a distance r in a time $\sim r/v_A$. For constant v_A , this scaling can be approximately recovered by taking the cosmic rays to diffuse isotropically with $D_{\text{cr}} \propto r$, the scaling that arises from equation (32) when $v_d r \gg D_0$. This self-confinement scenario is too simplistic, since in clusters field lines are tangled, v_A varies in space, and it is not known whether cosmic rays are primarily scattered by cosmic-ray-generated waves or by magnetohydrodynamic (MHD) turbulence excited by large-scale stirring of the intracluster plasma. It is not clear, however, how to improve upon equation (32). Self-confinement in the presence of tangled field lines is not well understood, and the standard theoretical treatment of scattering by MHD turbulence, which takes the fluctuations to have wave vectors directed along the background magnetic field, is known to be inaccurate (Bieber et al 1994, Chandran 2000, Yan & Lazarian 2004).³ A more definitive treatment must thus await further progress in our understanding of MHD turbulence and cosmic-ray transport. The value of D_{\parallel} is needed in the mixing length theory developed below. In analogy to equation (29), it is assumed that

$$D_{\parallel} = \frac{D_{\text{cr}}}{\theta}. \quad (33)$$

It is assumed that a black hole of mass M_{BH} at $r = 0$ accretes intracluster plasma at the Bondi (1952) rate

$$\dot{M} = \frac{\pi G^2 M_{\text{BH}}^2 \rho}{c_s^3} \quad (34)$$

corresponding to the average plasma parameters at $r = 0$, where c_s is the adiabatic sound speed. The resulting values of \dot{M} turn out to be a few $M_{\odot} \text{ yr}^{-1}$, which is much smaller

³See Farmer & Goldreich (2004) and Yan & Lazarian for a discussion of how MHD turbulence affects self-confinement, and Chandran et al (1999), Chandran (2000b), and Malyskin & Kulsrud (2001) for a discussion of the effects of magnetic mirrors.

than the mass inflow rate in the cooling-flow model (Fabian 1994). If one were to set $\langle v_r \rangle = -\dot{M}/4\pi r^2 \rho$ with \dot{M} of this order, the $\langle v_r \rangle$ terms in the average of equation (7) would be small compared to R for $r \gtrsim 1$ kpc. Because of this, $\langle \mathbf{v} \rangle$ is set to zero to simplify the model.

The mass accretion rate inferred from equation (34) is used to determine the cosmic-ray luminosity through the equation

$$L_{\text{cr}} = \eta \dot{M} c^2, \quad (35)$$

where η is a dimensionless efficiency factor. The spatial distribution of cosmic-ray injection into the ICM is not precisely known. Some clues are provided by radio observations, which show that cluster-center radio sources (CCRS) differ morphologically from radio sources in other environments. As discussed by Eilek (2004), roughly half of the CCRS in a sample of 250 sources studied by Owen & Ledlow (1997) are “amorphous,” or quasi-isotropic, presumably due to jet disruption by the comparatively high-pressure cluster-core plasma. With the exception of Hydra A, the CCRS in the Owen-Ledlow (1997) study are smaller than non-cluster-center sources, with most extending less than 50 kpc from the center of the host cluster (Eilek 2004). In this paper, the average cosmic-ray energy introduced into the intracluster medium per unit volume per unit time is taken to be

$$\langle \dot{E}_{\text{inj}} \rangle = S_0 e^{-r^2/r_s^2}, \quad (36)$$

where the constant r_s is a free parameter and the constant S_0 is determined from the equation $L_{\text{cr}} = 4\pi \int_0^\infty dr r^2 \langle \dot{E}_{\text{inj}} \rangle$ and equation (35).

The F_{cr} and W_{cr} terms are related to F and W by the assumption that convection is subsonic. The perturbation to the total pressure is then neglected, so that

$$\delta p_{\text{cr}} = -\delta p. \quad (37)$$

Since $\langle \mathbf{v} \rangle$ is also dropped, one has

$$F_{\text{cr}} = - \left(\frac{\gamma - 1}{\gamma_{\text{cr}} - 1} \right) F, \quad (38)$$

and

$$W_{\text{cr}} = -W. \quad (39)$$

The values of F and W are first obtained with the use of a local two-fluid mixing length theory that differs from the theory of paper I in that it accounts for heat and cosmic-ray transport along the magnetic field. Averages obtained in the local theory are denoted with the subscript L. These local quantities are then used as the basis for a nonlocal mixing

length theory. Average quantities in the nonlocal theory are weighted spatial averages of the corresponding quantities in the local theory, and are denoted with the subscript NL. The nonlocal quantities are used in the final model equations. The nonlocal theory is used because it is somewhat more realistic than the local theory and because it avoids the critical point discussed in paper I, which is related to the sensitivity of dF_L/dr to the fluid profiles when the intracluster medium is near marginal stability.

The local mixing length theory is derived as follows. Consider a fluid element in a convective region that starts at radial coordinate r_i at time $t = 0$ with initial fluid properties ρ_i , p_i , T_i , $p_{\text{cr},i}$, and $p_{\text{tot},i}$ equal to the average values at $r = r_i$. Suppose that the fluid element undergoes a displacement \mathbf{d} and is then mixed into the surrounding fluid, where $|\mathbf{d} \cdot \hat{\mathbf{r}}| = l > 0$,

$$l = \alpha r \tag{40}$$

is the mixing length, and the positive constant α is a free parameter. For the moment, it is assumed that $\alpha \ll 1$. Later, this assumption is relaxed—a well known inconsistency of local mixing length theory. The values of the fluid properties in the displaced fluid element just before it mixes into the surrounding medium are denoted ρ_f , p_f , T_f , $p_{\text{cr},f}$, and $p_{\text{tot},f}$. The rms value of δv_r is denoted u_L . The approximate time for the fluid element to undergo its displacement \mathbf{d} is

$$\Delta t = \frac{l}{u_L}. \tag{41}$$

Integrating equation (5), one obtains

$$\frac{\rho_f}{\rho_i} = e^{-\Gamma}, \tag{42}$$

where

$$\Gamma = \int_0^{\Delta t} dt \nabla \cdot \mathbf{v} \Big|_{\text{Lagr}}, \tag{43}$$

and

$$\int_0^{\Delta t} dt f \Big|_{\text{Lagr}} \equiv \int_0^{\Delta t} dt f(\mathbf{r}(t), t) \tag{44}$$

is the (Lagrangian) time integral of the (arbitrary) function f evaluated at the location of the moving fluid element $\mathbf{r}(t)$. Since the fluctuating quantities and α are treated as small, $|\Gamma| \ll 1$ and equation (42) can be written

$$\frac{\rho_f - \rho_i}{\rho_i} = -\Gamma. \tag{45}$$

It is assumed that the changes in p and p_{cr} in the moving fluid element during the time Δt due to H_{diss} , R , and \dot{E}_{inj} are small compared to the changes induced by the other terms in equations (7) and (8). Integrating equation (7) then yields

$$p_{\text{f}} - p_{\text{i}} = -\gamma \int_0^{\Delta t} dt p \nabla \cdot \mathbf{v} \Big|_{\text{Lagr}} + (\gamma - 1) \int_0^{\Delta t} dt \nabla \cdot (\kappa \cdot \nabla T) \Big|_{\text{Lagr}}. \quad (46)$$

To lowest order in $\delta p / \langle p \rangle$ and α ,

$$\int_0^{\Delta t} dt p \nabla \cdot \mathbf{v} \Big|_{\text{Lagr}} = p_{\text{i}} \Gamma. \quad (47)$$

When a fluid parcel of size l is displaced radially outwards, it remains magnetically connected to the same set of fluid elements to which it was initially connected (at least until it is mixed into the surrounding fluid, at which point it is assumed that the magnetic field in the fluid parcel is randomized). This is depicted schematically in figure 2. Because parallel conductivity acts to smooth out temperature variations along the magnetic field, the initial temperature of any fluid element in the parcel can be thought of as a weighted average of the temperature along the magnetic field out to some distance L_{\parallel} . Since the parallel conductivity in clusters is considerable and α is treated as small, L_{\parallel} can be taken to be larger than l . If one ignores temperature changes occurring outside the fluid parcel, then parallel conductivity acts to restore the fluid element's temperature towards its initial value, and the last term in equation (46) can be approximated as

$$(\gamma - 1) \int_0^{\Delta t} dt \nabla \cdot (\kappa \cdot \nabla T) \Big|_{\text{Lagr}} = -\frac{\xi \Delta t (\gamma - 1) \kappa_{\parallel} (T_{\text{f}} - T_{\text{i}})}{l^2}, \quad (48)$$

where ξ is a positive dimensionless constant, which is set equal to 1 in all of the numerical examples presented below. Equation (46) can thus be rewritten as

$$p_{\text{f}} - p_{\text{i}} = -\gamma \Gamma p_{\text{i}} - \frac{\xi \Delta t (\gamma - 1) \kappa_{\parallel} (T_{\text{f}} - T_{\text{i}})}{l^2}. \quad (49)$$

Parallel cosmic-ray diffusion is treated in the same way as parallel thermal conduction. Integrating equation (8) thus yields

$$p_{\text{cr,f}} - p_{\text{cr,i}} = -\gamma_{\text{cr}} \Gamma p_{\text{cr,i}} - \frac{\xi \Delta t D_{\parallel} (p_{\text{cr,f}} - p_{\text{cr,i}})}{l^2}. \quad (50)$$

Since fluctuating quantities and α are treated as small,

$$\frac{T_{\text{f}} - T_{\text{i}}}{T_{\text{i}}} \simeq \frac{p_{\text{f}} - p_{\text{i}}}{p_{\text{i}}} - \frac{\rho_{\text{f}} - \rho_{\text{i}}}{\rho_{\text{i}}}. \quad (51)$$

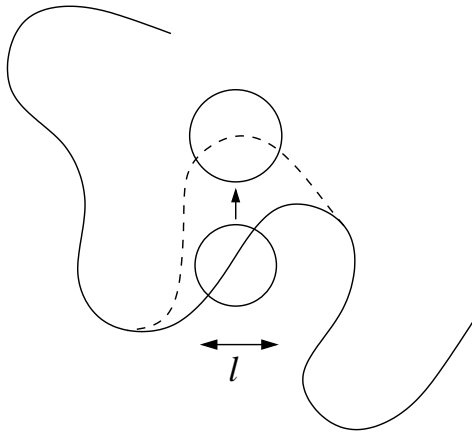


Fig. 2.— Schematic diagram of a rising fluid parcel. The solid line is a magnetic field line passing through the parcel’s initial location. The dashed line is an idealization of how the field line changes as a result of the fluid parcel’s displacement. In the diagram, velocities far from the fluid parcel are ignored, just as temperature variations far from the fluid parcel are neglected to derive the estimate in equation (48).

Equations (45), (49) and (51) combine to give

$$p_f - p_i = (\rho_f - \rho_i) \frac{p_i}{\rho_i} \left(\frac{\gamma + a_1}{1 + a_1} \right), \quad (52)$$

where

$$a_1 = \frac{\xi(\gamma - 1)\kappa_{\parallel}T_i}{lu_L p_i} \quad (53)$$

is roughly the ratio of Δt to the time for heat to diffuse a distance l along the magnetic field. When $a_1 \ll 1$ the thermal plasma expands adiabatically, and when $a_1 \gg 1$ the thermal plasma expands isothermally. With the aid of equation (45), equation (50) can be rewritten

$$p_{\text{cr},f} - p_{\text{cr},i} = \frac{(\rho_f - \rho_i)\gamma_{\text{cr}}p_{\text{cr},i}}{\rho_i(1 + a_2)}, \quad (54)$$

where

$$a_2 = \frac{\xi D_{\parallel}}{lu_L} \quad (55)$$

is approximately the ratio of Δt to the time for cosmic rays to diffuse a distance l along the magnetic field. When $a_2 \ll 1$, the cosmic rays expand adiabatically. When $a_2 \gg 1$ the cosmic ray pressure in the fluid element remains constant as the element is displaced, as in the linear Parker instability in the large- D_{\parallel} limit (Parker 1966, Shu 1974, Ryu et al 2003).

Since it is assumed that the convection is subsonic, the total pressure in the fluid element remains approximately the same as the average total pressure in the fluid element’s

surroundings. Thus, to lowest order in α

$$p_{\text{tot},f} - p_{\text{tot},i} = l \frac{d}{dr} \langle p_{\text{tot}} \rangle. \quad (56)$$

Since only the lowest-order terms have been kept, it is not necessary to specify in equation (56) whether $d\langle p_{\text{tot}} \rangle/dr$ is evaluated at r_i or $r_i + l$, so the argument of $d\langle p_{\text{tot}} \rangle/dr$ is not explicitly written. Arguments of average quantities are omitted in similar instances below. Adding equations (52) and (54) and using equation (56), one obtains

$$l \frac{d}{dr} \langle p_{\text{tot}} \rangle = \frac{A(\rho_f - \rho_i)}{\rho_i}, \quad (57)$$

where

$$A = \frac{(\gamma + a_1)p_i}{1 + a_1} + \frac{\gamma_{\text{cr}} p_{\text{cr},i}}{1 + a_2}. \quad (58)$$

The difference between the density inside the displaced fluid element and the average density of the surrounding medium is given by

$$\Delta\rho = \rho_f - \left(\rho_i + l \frac{d}{dr} \langle \rho \rangle \right). \quad (59)$$

Upon using equation (57) for $\rho_f - \rho_i$, one can rewrite equation (59) as

$$\Delta\rho = l \left(\frac{\langle \rho \rangle}{A} \frac{d}{dr} \langle p_{\text{tot}} \rangle - \frac{d}{dr} \langle \rho \rangle \right). \quad (60)$$

The fluid is stable if an outwardly displaced parcel is heavier than its surroundings. Since $dA/du_L > 0$ and $d\langle p_{\text{tot}} \rangle/dr < 0$, the quantity in brackets in equation (60) is positive for any $u_L > 0$ if it is positive as $u_L \rightarrow 0$. The stability criterion is thus (where from here on angle brackets around average quantities are dropped)

$$\frac{1}{p} \frac{dp_{\text{tot}}}{dr} - \frac{1}{\rho} \frac{d\rho}{dr} > 0. \quad (61)$$

From a physical standpoint, the $u_L \rightarrow 0$ limit is appropriate for the stability boundary because the turbulent velocity is small near marginal stability. Since it is assumed that the mean molecular weight μ is a constant, equation (61) can be rewritten

$$\frac{dp_{\text{cr}}}{dr} + nk_B \frac{dT}{dr} > 0 \quad (62)$$

[as in equation (4)], where $n = \rho/(\mu m_H)$ is the number density of thermal particles.

If the stability criterion is satisfied, the local convective velocity u_L is set equal to zero. Otherwise the fluid is convectively unstable and the value of u_L is found by solving the fourth-order polynomial equation

$$\frac{\rho u_L^2}{2} = \left| \frac{l \Delta \rho}{16} \frac{d\Phi}{dr} \right|. \quad (63)$$

Equation (63) states that the mean radial kinetic energy of the fluid element is the mixing length times the buoyancy force on the fully displaced parcel times the numerical factor of $1/16$ that is commonly used in one-fluid mixing length theory (Cox & Giuli 1968). Once u_L is found, $\rho_f - \rho_i$ and $p_f - p_i$ are determined from equations (52) and (57). The difference between the pressure inside the displaced fluid element and the average pressure of the surrounding material is

$$\Delta p = p_f - \left(p_i + l \frac{dp}{dr} \right). \quad (64)$$

It is assumed that half of the fluid at any radius r consists of rising fluid elements and half consists of sinking fluid elements, each of which contributes comparably to the internal-energy flux. These fluid elements originated over a range of initial radii r_i in the interval $(r-l, r+l)$, with pressure fluctuations whose magnitudes increase roughly linearly with $|r-r_i|$. Averaging over r_i , one obtains the estimate $F_L = c_{\text{avg}} u_L \Delta p / (\gamma - 1)$. The constant c_{avg} is chosen to be $1/2$ to match standard treatments of one-fluid mixing length theory (Cox & Giuli 1968),⁴ so that

$$F_L = \frac{u_L l}{2(\gamma - 1)} \left[\frac{p}{A} \left(\frac{\gamma + a_1}{1 + a_1} \right) \frac{dp_{\text{tot}}}{dr} - \frac{dp}{dr} \right]. \quad (65)$$

The typical value of $\nabla \cdot \mathbf{v}$, denoted $(\text{div } v)$, is given by

$$(\text{div } v) = \frac{1}{\Delta t} \int_0^{\Delta t} dt \nabla \cdot \mathbf{v} \Big|_{\text{Lagr}} = \frac{u_L \Gamma}{l}. \quad (66)$$

The value of W_L is estimated using the same factor of $1/2$ employed in estimating F_L , so that $W_L = \Delta p (\text{div } v) / 2$, or

$$W_L = -\frac{u_L l}{2A} \left[\frac{p}{A} \left(\frac{\gamma + a_1}{1 + a_1} \right) \frac{dp_{\text{tot}}}{dr} - \frac{dp}{dr} \right] \frac{dp_{\text{tot}}}{dr}. \quad (67)$$

Note that in the limit $a_2 \rightarrow \infty$, $A = p(\gamma + a_1)/(1 + a_1)$ and $\Delta p = l dp_{\text{cr}}/dr$. This is because in this limit $p_{\text{cr},f} = p_{\text{cr},i}$. Thus, since $p_{\text{tot},f} = p_{\text{tot}}(r_i + l)$, Δp equals the change in the average cosmic-ray pressure of the surrounding fluid.

⁴In paper I, c_{avg} was instead chosen to match values in the literature for the constant c_1 defined in equation (85) below.

In the study of Ulrich (1976), the nonlocal heat flux is given by a weighted spatial average of the heat flux obtained from local mixing length theory. The same approach is adopted here, so that

$$F_{\text{NL}}(z) = \int_{-\infty}^{\infty} dz_1 F_{\text{L}}(z_1) \psi_F(z - z_1), \quad (68)$$

$$W_{\text{NL}}(z) = \int_{-\infty}^{\infty} dz_1 W_{\text{L}}(z_1) \psi_W(z - z_1), \quad (69)$$

and

$$u_{\text{NL}}(z) = \int_{-\infty}^{\infty} dz_1 u_{\text{L}}(z_1) \psi_u(z - z_1), \quad (70)$$

where $dz = dr/H_p$, and H_p is the pressure scale height. In this paper, H_p is replaced by r , so that

$$z = \ln \left(\frac{r}{r_{\text{ref}}} \right), \quad (71)$$

where r_{ref} is an unimportant constant. Different forms for the kernel function ψ_F were considered by Ulrich (1976). Here, the following values are adopted:

$$\psi_u(x) = \psi_F(x) = \begin{cases} \alpha^{-1} e^{-x/\alpha} & \text{if } x > 0 \\ 0 & \text{if } x \leq 0 \end{cases}, \quad (72)$$

and

$$\psi_W(x) = \begin{cases} \alpha_W^{-1} e^{-x/\alpha_W} & \text{if } x > 0 \\ 0 & \text{if } x \leq 0 \end{cases}. \quad (73)$$

Equations (68) through (73) are equivalent to the differential equations

$$\alpha r \frac{dF_{\text{NL}}}{dr} + F_{\text{NL}} = F_{\text{L}}, \quad (74)$$

$$\alpha r \frac{du_{\text{NL}}}{dr} + u_{\text{NL}} = u_{\text{L}}, \quad (75)$$

and

$$\alpha_W r \frac{dW_{\text{NL}}}{dr} + W_{\text{NL}} = W_{\text{L}}. \quad (76)$$

For $r > r_{\text{conv}}$, where r_{conv} is the largest radius at which the fluid is convective, $F_{\text{NL}} \propto r^{-1/\alpha}$. When F and W are set equal to F_{NL} and W_{NL} in equation (22), the term containing F_{NL} is $\propto r^{-1-1/\alpha}$ for $r > r_{\text{conv}}$. To obtain the same scaling for the term containing W_{NL} in equation (22), the value of α_W is determined from the equation

$$\alpha_W^{-1} = \alpha^{-1} + 1. \quad (77)$$

Equations (72) and (73) represent a one-sided average, in the sense that the nonlocal flux at radius r depends only on the fluid quantities at smaller radii. A more realistic two-sided average would correspond to second-order differential equations for F_{NL} , u_{NL} , and W_{NL} (Travis & Matsushima 1973, Ulrich 1976). The one-sided average is adopted for convenience. [The reason is that the second-order differential equations have homogeneous solutions that grow with r , which make it more difficult to guess the boundary conditions at $r = 0$ when the equations are solved numerically using the shooting method described below.] A more sophisticated nonlocal theory could be developed along different lines (see e.g. Ulrich 1976, Xiong 1991, Grossman, Narayan, & Arnett 1993), but is beyond the scope of this paper.

The average of the viscous dissipation term is set equal to

$$H_{\text{diss}} = \frac{0.42\rho u_{\text{rms}}^3}{l}, \quad (78)$$

where

$$u_{\text{rms}} = \sqrt{3} u_{\text{NL}} \quad (79)$$

is the rms three-dimensional velocity corresponding to the rms radial velocity represented by u_{NL} , and the constant 0.42 is taken from direct numerical simulations of compressible magnetohydrodynamic turbulence (Haugen, Brandenburg, & Dobler 2004).⁵ [It turns out that in the solutions presented below, H_{diss} is much smaller than the other turbulent heating terms (see footnote 4 of paper I for an explanation).]

Setting $F = F_{\text{NL}}$ and $W = W_{\text{NL}}$, one can rewrite equations (20), (22), and (23) as⁶

$$\frac{dp_{\text{tot}}}{dr} = -\rho \frac{d\Phi}{dr}, \quad (80)$$

$$\frac{1}{r^2} \frac{d}{dr} (r^2 F_{\text{NL}}) = -W_{\text{NL}} + H_{\text{diss}} + \frac{1}{r^2} \frac{d}{dr} \left(r^2 \kappa_T \frac{dT}{dr} \right) - R, \quad (81)$$

and

$$-\left(\frac{\gamma - 1}{\gamma_{\text{cr}} - 1} \right) \frac{1}{r^2} \frac{d}{dr} (r^2 F_{\text{NL}}) = W_{\text{NL}} + \frac{1}{(\gamma_{\text{cr}} - 1)r^2} \frac{d}{dr} \left(r^2 D_{\text{cr}} \frac{dp_{\text{cr}}}{dr} \right) + \dot{E}_{\text{inj}}. \quad (82)$$

Equations (74), (75), (76), (80), (81), and (82) form a system of four first-order equations and two second-order equations for the six variables ρ , T , p_{cr} , F_{NL} , u_{NL} , and W_{NL} .

⁵The constant 0.42 is obtained by taking the mixing length l to correspond to π/k_p in the simulations of Haugen et al (2004), where k_p is the wave number at which $kE(k)$ peaks, and $E(k)$ is the power spectrum of the turbulent velocity.

⁶See paper I for a discussion of the $p_{\text{cr}} \rightarrow 0$ limit and the need to include $\langle v_r \rangle$ to treat this limit properly.

Eight boundary conditions are required to specify a solution. Two boundary conditions are obtained by imposing a density ρ_{outer} and temperature T_{outer} at radius r_{outer} . Two boundary conditions are obtained by taking dT/dr and dp_{cr}/dr to vanish at the origin. Three additional boundary conditions are obtained by requiring dF_{NL}/dr , dW_{NL}/dr , and du_{NL}/dr to be finite at the origin. This leads to the condition at $r = 0$ that $F_{\text{NL}} = F_{\text{L}}$, $W_{\text{NL}} = W_{\text{L}}$, and $u_{\text{NL}} = u_{\text{L}}$. (Since dT/dr and dp_{cr}/dr vanish at $r = 0$, the cluster is marginally stable at $r = 0$, and F_{L} , W_{L} , and u_{L} vanish at $r = 0$.) The eighth boundary condition is obtained by assuming that $p_{\text{cr}} \rightarrow 0$ as $r \rightarrow \infty$. This condition is translated into a condition on p_{cr} at r_{outer} as follows. The value of r_{outer} is chosen to be significantly greater than r_s and much greater than D_0/v_d , so that for $r > r_{\text{outer}}$, \dot{E}_{inj} is negligible and $D_{\text{cr}} \simeq v_d r$.⁷ In addition, r_{outer} is taken to lie outside r_{conv} , the largest radius at which the intracluster medium is convectively unstable, so that $F_{\text{NL}} = F_{\text{outer}}(r/r_{\text{outer}})^{-1/\alpha}$ and $W_{\text{NL}} = W_{\text{outer}}(r/r_{\text{outer}})^{-1-1/\alpha}$ for $r > r_{\text{outer}}$, where F_{outer} and W_{outer} are the values of F_{NL} and W_{NL} at $r = r_{\text{outer}}$. Solving equation (82) and requiring that $p_{\text{cr}} \rightarrow 0$ as $r \rightarrow \infty$, one finds that for $r \geq r_{\text{outer}}$

$$\frac{dp_{\text{cr}}}{dr} = \frac{\chi}{v_d r^{1+1/\alpha}} - \frac{2p_{\text{cr}}}{r}, \quad (83)$$

where

$$\chi = (2\alpha - 1)(\gamma - 1)F_{\text{outer}}r_{\text{outer}}^{1/\alpha} + \alpha(\gamma_{\text{cr}} - 1)W_{\text{outer}}r_{\text{outer}}^{1+1/\alpha}. \quad (84)$$

Equation (83) applied at $r = r_{\text{outer}}$ provides the eighth boundary condition. Numerical solutions are obtained using a shooting method. Values are guessed for ρ , T , and p_{cr} at $r = 0$ and the equations are integrated from 0 to r_{outer} . The guesses are then updated using Newton’s method until the three boundary conditions at r_{outer} are met.

Figure 3 compares three model solutions to x-ray observations of the Virgo cluster, Perseus cluster, and Abell 478. In all three solutions, the following parameters are used: $M_{\text{BH}} = 10^9 M_{\odot}$, $\eta = 0.01$, $\gamma = 5/3$, $\gamma_{\text{cr}} = 4/3$, $\alpha = 0.5$, $r_s = 25$ kpc, $v_d = 100$ km/s, $D_0 = 10^{28}$ cm²/s, $\theta = 0.2$, $v_g = 400$ km/s, $r_g = 1$ kpc, and $r_{\text{outer}} = 100$ kpc. The only differences between the model solutions are the parameters describing the dark-matter density profiles, which are taken from the literature (see table 1), and the values of ρ_{outer} and T_{outer} , which are chosen to match the observations at $r = r_{\text{outer}}$ in Perseus and A478 and at $r = 61$ kpc (the outermost data point) in the Virgo cluster.

The deprojected temperature and density data for A 478 are provided by S. Allen (private communication; see Sun et al 2003) and assume $\Omega_0 = 0.3$, $\Omega_{\Lambda,0} = 0.7$, and $H_0 = 70$ km s⁻¹Mpc⁻¹. The deprojected temperature and density data for Perseus are provided

⁷The case $v_d = 0$ requires a different approach and is not treated in this paper.

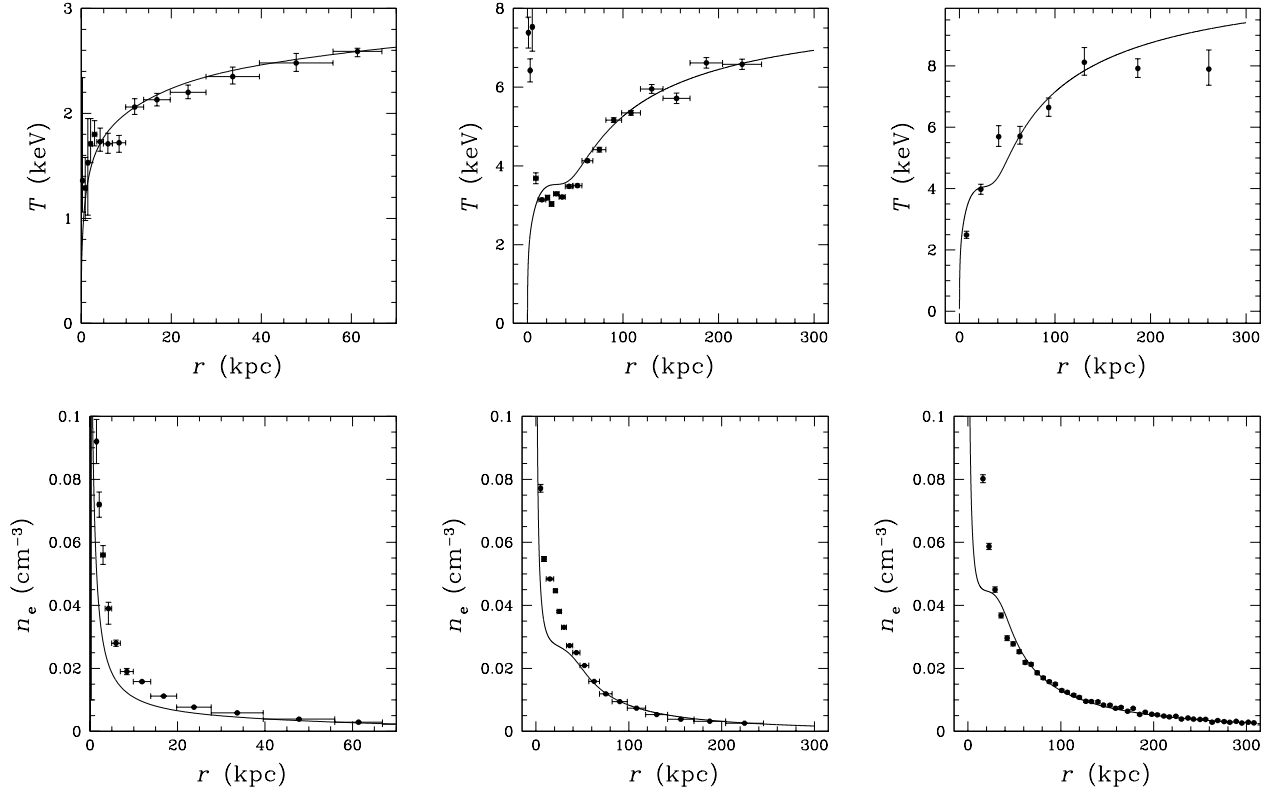


Fig. 3.— First, second, and third columns correspond to Virgo, Perseus, and Abell 478, respectively.

by E. Churazov (private communication) and are based on the observations of Churazov et al (2003), but with $H_0 = 71 \text{ km s}^{-1}\text{Mpc}^{-1}$ instead of the value $H_0 = 50 \text{ km s}^{-1}\text{Mpc}^{-1}$ used in the original article. The central peak in the Perseus temperature data is due to the hard power-law spectrum of the central active galaxy NGC 1275 (E. Churazov, private communication). The data for Virgo are from Matshushita et al (2002).

Figure 4 shows the cosmic-ray pressure divided by the plasma pressure and the rms turbulent velocity for the three model solutions plotted in figure 3. For reference, in the model solution for the Virgo cluster, $\dot{M} = 0.081M_\odot \text{ yr}^{-1}$, $L_{\text{cr}} = 4.6 \times 10^{43} \text{ ergs/s}$, the radiative luminosity out to 100 kpc is $1.2 \times 10^{43} \text{ erg/s}$, and the radiative luminosity out to 300 kpc is $2.5 \times 10^{43} \text{ erg/s}$. In the model solution for the Perseus cluster, $\dot{M} = 1.7M_\odot \text{ yr}^{-1}$, $L_{\text{cr}} = 9.8 \times 10^{44} \text{ ergs/s}$, the radiative luminosity out to 100 kpc is $4.1 \times 10^{44} \text{ erg/s}$, and the radiative luminosity out to 300 kpc is $1.0 \times 10^{45} \text{ erg/s}$. In the model solution for the A 478, $\dot{M} = 3.8M_\odot \text{ yr}^{-1}$, $L_{\text{cr}} = 2.2 \times 10^{45} \text{ ergs/s}$, the radiative luminosity out to 100 kpc

Table 1: NFW parameters and redshift.

Cluster	r_s (kpc)	c	z	reference
Virgo	560	2.77	(0.0040)	1
Perseus	500	3.86	0.018	2
A 478	610	3.88	0.088	3

NOTE.—redshift (z) of Virgo is set equal to $H_0 d/c$, with $d = 17$ Mpc and $H_0 = 70$ km s $^{-1}$ Mpc $^{-1}$.

REFERENCES.—(1) McLaughlin (1999); (2) Ettori, Fabian, & White (1998) (3) Schmidt, Allen, & Fabian (2004).

is 1.0×10^{45} erg/s, and the radiative luminosity out to 300 kpc is 2.8×10^{45} erg/s.

4. Discussion

Active galactic nuclei offer a promising solution to the cooling-flow problem on both observational and theoretical grounds: there is an active radio source at the center of almost every strongly cooling cluster (Eilek 2004), and AGN feedback in combination with thermal conduction can lead to globally stable equilibria (Rosner & Tucker 1989, Ruszkowski & Begelman 2002). The recent detection of moderately subsonic plasma motions in the Perseus cluster (Churazov et al 2004) suggests that turbulent heating is also important for the intracluster medium. The model presented in this paper connects AGN feedback to turbulent heating. It is assumed that radiative cooling is balanced by a combination of turbulent heating and thermal conduction. The turbulence arises from convection, which is driven by the cosmic-ray pressure gradient. The cosmic rays are produced by a central radio source, and it is assumed that the cosmic rays mix into the thermal plasma. The model treats convection using a nonlocal two-fluid mixing length theory. In some ways the model is analogous to a convective star, with cosmic rays playing the role of photons.

4.1. How successful is the model?

The model is compared to observations in figure 3. For Perseus, the model temperature profile has a plateau-like feature at $r \sim 20 - 30$ kpc, which also appears in the observational

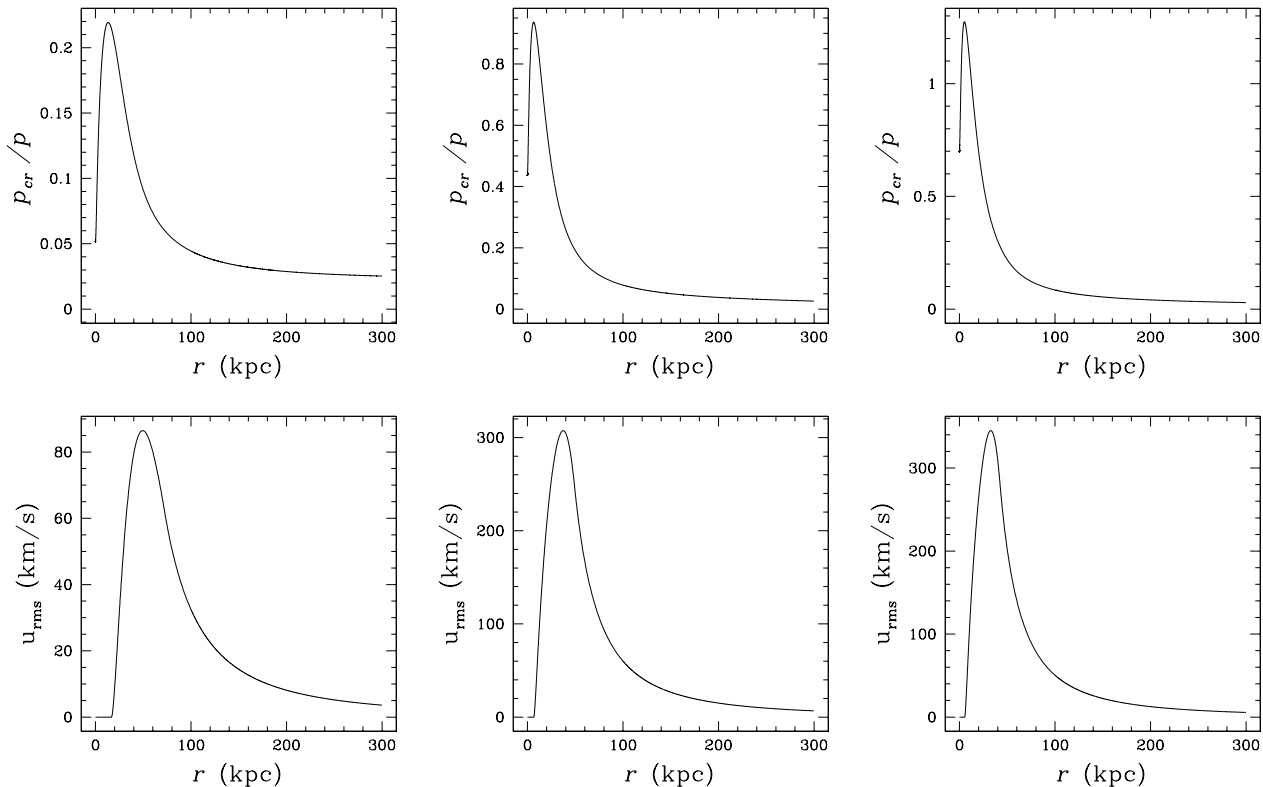


Fig. 4.— First, second, and third columns correspond to Virgo, Perseus, and Abell 478, respectively.

data. This local flattening of the temperature profile makes the intracluster medium more convectively unstable, and is associated with large turbulent velocities. The model predicts maximum turbulent velocities of order 300 km/s in Perseus, similar in magnitude to the plasma velocities inferred by Churazov et al (2004). It should be emphasized that the three solutions shown in figure 3 are all based on a single choice of “round-number” values for the model’s free parameters, as opposed to values that were fine-tuned to fit the data. Given the lack of fine tuning, the model is reasonably successful at matching the observations, although there are some important discrepancies. The model overestimates the temperature in A478 at $r \sim 200 - 300$ kpc and underestimates the electron density at $r \sim 10 - 30$ kpc in each cluster. This density discrepancy persists for all values of the model’s free parameters that have been investigated thus far and may be related to the assumption that the cosmic rays are well mixed into the thermal plasma, as discussed further in the next section.

4.2. Mixing of cosmic rays into the thermal plasma.

The mixing-length theory developed in section 3 treats the turbulent fluctuations $\delta\rho$, δp , and δp_{cr} as small quantities. This entails the assumption that the cosmic rays are well mixed into the thermal plasma (since at fixed r there is little variation in p_{cr}/p). However, roughly one-fourth of the clusters in the Chandra archive show clear evidence of x-ray cavities, which are typically ~ 10 kpc in radius at a projected distance of ~ 20 kpc from the cluster center (Birzan et al 2004). Many of these cavities are associated with enhanced synchrotron emission, suggesting that the cavities are cosmic-ray bubbles inflated by the central radio source. These cavities indicate that, at least within the central ~ 30 kpc of many clusters, the cosmic rays are not well mixed into the thermal plasma and $\delta\rho \sim \langle\rho\rangle$, $\delta p_{\text{cr}} \sim \langle p_{\text{cr}}\rangle$, etc. It is likely that the cosmic rays are better mixed into the thermal plasma at larger r , owing to the combined action of cosmic-ray diffusion, instabilities of bubble/plasma interfaces, and turbulent mixing, but in this paper no attempt is made to quantify the degree of mixing as a function of radius.

In low- p_{cr} regions within the central 30 kpc, cosmic rays are less able to support the plasma against gravity than in the model of this paper, and $|dp/dr|$ has to be larger. Accounting for this properly would likely increase n_e in parts of the central region, and possibly increase the plasma mass in the central region. Even if the plasma mass profile remained the same but the electrons were confined primarily to some fraction of the volume, the x-ray surface brightness would increase because $R \propto n_e^2$. A larger surface brightness would in turn increase the observationally inferred value of the volume-averaged electron density. A proper treatment of incomplete mixing might thus resolve the discrepancy between the model density profile and the observations, but further work is needed to investigate this possibility.

4.3. Relation to turbulent heating models

Several studies have shown that for plausible values of the turbulent velocity and velocity correlation length, heating from turbulent diffusion and viscous dissipation of turbulent motions can balance radiative cooling in clusters with a wide range of average temperatures (Kim & Narayan 2003, Voigt & Fabian 2004, Dennis & Chandran 2005). The main challenge for turbulent heating models is to explain how u_{rms} gets fine-tuned to the value required for turbulent heating to balance radiative cooling. The AGN-driven convection model presented in this paper offers an explanation for this fine-tuning by linking the turbulence amplitude to the cosmic-ray luminosity L_{cr} of the central radio source. The Bondi accretion rate \dot{M}_{Bondi} is a decreasing function of the specific entropy of the central plasma, s_0 , and

$L_{\text{cr}} \propto \dot{M}_{\text{Bondi}} c^2$. Thus, if u_{rms} were so large that the total heating exceeded radiative cooling, then s_0 would grow and \dot{M}_{Bondi} and L_{cr} would decrease. This would in turn reduce p_{cr} and thereby reduce u_{rms} , since it is the cosmic-ray pressure gradient that drives the convection.

4.4. Mixing of heavy elements

Galaxy clusters with short central cooling times (“cooling-core clusters”) have centrally peaked heavy-element abundances (Fukazawa et al 1996, DeGrandi & Molendi 2001). While the iron abundance peaks sharply towards $r = 0$ in such clusters, the abundance of oxygen is essentially flat in the central region. Since oxygen is effectively produced by type II SN but not by type I SN, the flat oxygen-abundance profile indicates that heavy element enrichment in cluster cores is dominated by type I SN.⁸ For plausible models of the history of the SN Ia rate in the central CD galaxy, more than 5 Gyr is typically required for SN Ia to enrich the plasma in cooling-core clusters within the central ~ 50 kpc to the observed levels (Böhringer et al 2004b). This implies that turbulence can not transport metals out of the central 50 kpc on a time scale much shorter than 5 Gyr. At the same time, the abundance peak is spread out over a larger region than the stars of the cD galaxy. Thus, some mixing out of the central region is required (Böhringer et al 2004a).

The eddy diffusivity in hydrodynamic turbulence is

$$D_{\text{eddy}} = c_1 u_{\text{rms}} l_0, \quad (85)$$

where u_{rms} is the rms turbulent velocity and l_0 is the dominant length scale (outer scale) of the turbulent velocity. Values in the literature for the dimensionless constant c_1 range from 0.06 to 0.18 (see Dennis & Chandran 2005), although it should be noted that these values depend on the definition employed for l_0 . [These values for c_1 are $\ll 1$ because in a 3D random walk the diffusion coefficient is $(\Delta x)^2/6\Delta t$ instead of just $(\Delta x)^2/\Delta t$, where Δx is the step size and Δt is the time between steps (Chandrasekhar 1943).] If $l_0 = \alpha r$, then the time scale for elements to be mixed out of the region interior to radius r , $t_{\text{mix}} = r^2/D_{\text{eddy}}$, is

$$t_{\text{mix}} = 5 \times 10^9 \text{ yr} \left(\frac{r}{50 \text{ kpc}} \right) \left(\frac{200 \text{ km/s}}{u_{\text{rms}}} \right) \left(\frac{0.1}{c_1} \right) \left(\frac{0.5}{\alpha} \right). \quad (86)$$

Some studies have argued that in MHD turbulence, magnetic tension reduces D_{eddy} relative

⁸In the bulk of a cluster’s volume, the iron-to-silicon ratio is typical of type II supernovae, and it is generally believed that type II SN dominate the heavy element enrichment (Finoguenov et al 2000, DeGrandi & Molendi 2001).

to the estimate in equation (85) (Vainshtein & Rosner 1991, Cattaneo 1994), but this claim has been recently challenged (Cho et al 2003).

Equation (86) indicates that mixing times are comparable to enrichment times for plausible turbulence parameters, although a more careful analysis is needed to determine whether the AGN-driven convection model is consistent with enrichment-time constraints. Two factors that would affect such an analysis are the following. First, the turbulent velocity peaks in the central region, dropping significantly outside of the central 50 kpc in the solutions plotted in figure 4. This allows for efficient mixing within the central 50-100 kpc, but reduces the rate at which metals are mixed out to larger radii. Second, the observed incomplete mixing of cosmic rays in the central ~ 30 kpc discussed above may limit the ability of rising cosmic-ray-dominated bubbles in the very central region to carry enriched plasma outwards (see, e.g., Brügggen et al 2002).

4.5. Implications for diffuse γ -ray emission

Cosmic-ray protons in the intracluster medium interact with thermal-plasma nucleons to produce pions. Neutral pions then decay into gamma rays. In this section, the results of Pfrommer & Ensslin (2004) are used to calculate the gamma-ray fluxes that would result from the model solutions for $p_{\text{cr}}(r)$ and $n_e(r)$ presented in section 3. The cosmic-ray-proton distribution function (number of cosmic-ray protons per unit volume per unit momentum), denoted f , is assumed to be

$$f(p) = \tilde{n}_{\text{cr}}(r) \left(\frac{pc}{1 \text{ GeV}} \right)^{-\alpha_p} \frac{c}{1 \text{ GeV}}, \quad (87)$$

where the constant α_p is a free parameter satisfying $2 < \alpha_p < 3$. At the risk of notational confusion, p in equation (87) is the cosmic-ray momentum, even though p was previously defined to be the plasma pressure. It is assumed that all of the cosmic-ray pressure arises from cosmic-ray protons. The value of $\tilde{n}_{\text{cr}}(r)$ corresponding to the model solutions of section 3 is thus determined by equating the value of $p_{\text{cr}}(r)$ in the model solutions to $\int_0^\infty dp f v p / 3$, where v is the cosmic-ray speed at momentum p . This gives

$$\tilde{n}_{\text{cr}}(r) = \frac{6p_{\text{cr}}(r)}{m_p c^2} \left(\frac{m_p c^2}{1 \text{ GeV}} \right)^{\alpha_p - 1} \left[B \left(\frac{\alpha_p - 2}{2}, \frac{3 - \alpha_p}{2} \right) \right]^{-1}, \quad (88)$$

where m_p is the proton mass and $B(z, w) = \int_0^1 t^{z-1} (1-t)^{w-1}$ is the beta function. Because $2 < \alpha_p < 3$, the cosmic-ray pressure and energy density are finite even though the power-law scaling in equation (87) is taken to apply for $p \in (0, \infty)$. Once $\tilde{n}_{\text{cr}}(r)$ is determined, the

observed flux of gamma rays is obtained using equations (19) through (21) of Pfrommer & Ensslin (2004) and the model solutions for $n_e(r)$. The flux at Earth of photons with energies exceeding 100 MeV emitted by the central 300 kpc of each cluster is listed in table 2 for four values of the parameter α_p , along with EGRET upper limits from Reimer et al (2003). The predicted fluxes are all below the EGRET upper limits. However, the fluxes equal or exceed the expected sensitivity to photons above 100 MeV of a future GLAST two-year all-sky survey [$2 \times 10^{-9} \text{ cm}^{-2} \text{ s}^{-1}$; Gehrels & Michelson (1999)]. Future GLAST observations will thus provide an important test of the AGN-driven convection model.

Table 2: Predicted gamma-ray photon fluxes and EGRET upper limits

Cluster	Predicted flux above 100 MeV ($10^{-8} \text{ cm}^{-2} \text{ s}^{-1}$)				EGRET flux above 100 MeV ($10^{-8} \text{ cm}^{-2} \text{ s}^{-1}$)
	$\alpha_p = 2.1$	$\alpha_p = 2.3$	$\alpha_p = 2.5$	$\alpha_p = 2.7$	
Virgo	0.36	0.55	0.45	0.27	< 2.18
Perseus	1.8	2.7	2.2	1.3	< 3.72
A 478	0.27	0.41	0.33	0.20	< 5.14

Two sources of error in the predicted gamma-ray flux should be noted. As discussed previously, the model underestimates the plasma density within the central ~ 30 kpc, which acts to decrease the predicted gamma-ray flux. On the other hand, the inaccurate assumption that the cosmic rays are well mixed into the thermal plasma within the central ~ 30 kpc acts to increase the predicted gamma-ray flux.

Hadronic interactions between cosmic-ray protons and thermal plasma also generate charged pions, which decay into secondary electrons and neutrinos. Pfrommer & Ensslin (2004) have calculated upper limits for the energy density of cosmic-ray protons in the Perseus cluster based on the radio emission from secondary electrons. Their upper limits are well below the peak values presented in figure 4, but depend upon the assumed magnetic field strength, the power-law index α_p , and the spatial variation of p_{cr} . This may be a problem for the model of this paper, and warrants further investigation.

4.6. Convection and the intracluster dynamo

The origin of intracluster magnetic fields remains a mystery. If they originate from dynamo action in the intracluster medium, AGN-driven convection provides a means for generating the needed turbulence in cluster cores.

I thank Eliot Quataert, Ian Parrish, and Jim Stone for discussions of the influence of parallel heat transport on convection, Steve Allen for providing the data for A478, Eugene Churazov for providing the data for the Perseus cluster, and Steve Cowley, Eric Blackman, Aristotle Socrates, and Olaf Reimer for other interesting discussions. This work was supported by the National Aeronautics and Space Administration under Astrophysical-Theory-Program grant NNG05GH39G issued by the Office of Space Science. This work was also supported by DOE grant DE-FG02-01ER54658 at the University of Iowa.

REFERENCES

- Balbus, S. 2001, *ApJ*, 562, 909
- Begelman, M. C. 2001, in ASP Conf. Proc., 240, *Gas and Galaxy Evolution*, ed. J. E. Hibbard, M. P. Rupen, & J. H. van Gorkom (San Francisco: ASP), 363
- Begelman, M. C. 2002, in ASP Conf. Proc., 250, *Particles and Fields in Radio Galaxies*, ed. R. A. Laing, & K. M. Blundell (San Francisco: ASP), 443
- Binney, J., & Tabor, G. 1995, *MNRAS*, 276, 663
- Birzan, L., Rafferty, D., McNamara, B., Wise, M., & Nulsen, P. 2004, *ApJ*, 607, 800
- Böhringer, H. et al 2001, *A&A*, 365, L181
- Böhringer, H., Matsushita, K., Churazov, E., & Finoguenov, A. 2004a, in *The Riddle of Cooling Flows and Clusters of Galaxies*, ed. Reiprich, T., Kempner, J., & Soker, N., E3, <http://www.astro.virginia.edu/coolflow/proc.php>
- Böhringer, H., Matsushita, K., Churazov, E., Finoguenov, A., & Ikebe, Y. 2004b, *A&A*, 416, L21
- Böhringer, H., & Morfill, G. 1988, *ApJ*, 330, 609
- Bondi, H. 1952, *MNRAS*, 112, 159
- Borgani, S., Murante, G., Springel, V., Diaferio, A., Dolag, K., Moscardini, L., Tormen, G., Tornatore, L., & Tozzi, P. 2004, *MNRAS*, 348, 1078
- Brüggen, M 2003, *ApJ*, 592, 839

- Brüggen, M., Kaiser, C., Churazov, E., & Ensslin, T. 2002, MNRAS, 331, 545
- Cattaneo, F. 1994, ApJ, 434, 200
- Cen, R. 2005, ApJ, 620, 191
- Chandran, B. 2000a, Phys. Rev. Lett., 85, 4656
- Chandran, B. 2000b, ApJ, 529, 513
- Chandran, B. 2004, ApJ, 616, 169 (Paper I)
- Chandran, B., & Cowley, S. 1998, Phys. Rev. Lett., 80, 3077
- Chandran, B., Cowley, S., Ivanushkina, M., & Sydora, R. 1999, ApJ, 525, 638
- Chandran, B., Maron, J. 2004, ApJ, 602, 170
- Chandrasekhar, S. 1943, Rev. Mod. Phys., 15, 1
- Cho, J., Lazarian, A., Honein, A., Knaepen, B., Kassinos, S., and Moin P. 2003, ApJ, 589, L77
- Churazov, E., Brüggen, M., Kaiser, C., Böhringer, H., & Forman, W. 2001, ApJ, 554, 261
- Churazov, E., Forman, W., Jones, C., & Böhringer, H. 2003, ApJ, 590, 225
- Churazov, E., Forman, W., Jones, C., Sunyaev, R., & Böhringer, H. 2004, MNRAS, 347, 29
- Churazov, E., Sunyaev, R., Forman, W., & Böhringer, H. 2002, MNRAS, 332, 729
- Ciotti, L., & Ostriker, J. 1997, ApJ, 487, L105
- Ciotti, L., & Ostriker, J. 2001, ApJ, 551, 131
- Ciotti, L., & Ostriker, J., & Pellegrini, S. 2004, in *Plasmas in the Laboratory and in the Universe: New Insights and New Challenges*, American Institute of Physics Conference Series, vol. 703, p. 367
- Cox, J., & Guili, R. 1968, *Principles of Stellar Structure* (New York: Gordon and Breach)
- Crawford, C. S., Allen, S. W., Ebeling, H., Edge, A. C., & Fabian A. C. 1999, MNRAS, 306, 857
- Dennis, T., & Chandran, B. 2005, 621, ...
- Dolag, K., Jubelgas, M., Springel, V., Borgani, S., Rasia, E. 2004, ApJ, 606, 97
- Drury, L., & Volk, H. 1981, ApJ, 248, 344
- Eilek, J. 2004, in *The Riddle of Cooling Flows and Clusters of Galaxies*, ed. Reiprich, T., Kempner, J., & Soker, N., E13, <http://www.astro.virginia.edu/coolflow/proc.php>
- Ettori, S., Fabian, A., & White, D. 1998, MNRAS, 300, 837

- Farmer, A., & Goldreich, P. 2004, ApJ, 604, 671
- Fabian, A. C. 1994, Ann. Rev. Astr. Astrophys., 32, 277
- Fabian, A. C., Sanders, J., Allen, S., Crawford, C., Iwasawa, K., Johnstone, M., Schmidt, R., & Taylor, G. 2003, MNRAS, 344, L43
- Finoguenov, A., Arnaud, M., & David, L. P. 2001, ApJ, 555, 191
- Gehrels, N., & Michelson, P. 1999, Astroparticle Phys., 11, 277
- Goldreich, P. & Sridhar, S. 1995, ApJ, 438, 763
- Grossman, S., Narayan, R., & Arnett, D. 1993, ApJ, 407, 284
- Haugen, N., Brandenburg, A., & Dobler, W. 2004, Phys. Rev. E, 70, 016308
- Hoeft, M., & Brüggén, M. 2004, ApJ, 617, 896
- Kim, W., & Narayan, R. 2003, ApJ, 596, L13
- Kronberg, P. 1994, Rep. Prog. Phys., 57, 325
- Jones, T., & Kang, H. 1990, ApJ, 363, 499
- Lewis, G. F., Babul, A., Katz, N., Quinn, T., Hernquist, L., & Weinberg, D. 2000, ApJ, 536, 623
- Loewenstein, M., & Fabian, A. 1990, MNRAS, 242, 120
- Loewenstein, M., Zweibel, E., & Begelman, M. 1991, ApJ, 377, 392
- Malyshkin, L., & Kulsrud, R. 2001, ApJ, 549, 402
- Maron, J., Chandran, B., & Blackman, E. 2004, Phys. Rev. Lett., 92, id. 045001
- McLaughlin, D. 1999, ApJ, 512, L9
- McNamara, B. 2004, in *The Riddle of Cooling Flows and Clusters of Galaxies*, ed. Reiprich, T., Kempner, J., & Soker, N. (Charlottesville: Univ. Virginia), E51, <http://www.astro.virginia.edu/co>
- McNamara, B. R., Wise, M. W., & Murray, S. S. 2004, ApJ, 601, 173
- McNamara, B. R., Wise, M. W., Nulsen, P. E. J., David, L. P., Carilli, C. L., Sarazin, C. L., O’Dea, C. P., Houck, J., Donahue, M., Baum, S., Voit, M., O’Connell, R. W., Koekemoer, A. 2001, ApJL, 562, 149
- Molendi, S., & Pizzolatao, F. 2001, ApJ, 560, 194
- Nagai, D., & Kravtsov, A. 2004, astro-ph/0404350
- Navarro, J., Frenk, C., & White, S. 1997, ApJ, 490, 493
- Narayan, R., & Medvedev, M. 2001, ApJ, 562, 129

- Nulsen, P. 2004, in *The Riddle of Cooling Flows and Clusters of Galaxies*, ed. Reiprich, T., Kempner, J., & Soker, N., E30, <http://www.astro.virginia.edu/coolflow/proc.php>
- Owen, F., & Ledlow, M. 1997, *ApJS*, 108, 410
- Parker, E. 1966, *ApJ*, 145, 811
- Pen, U., Matzner, C., & Wong, S. 2003, *ApJ*, 596, L207
- Peterson, J. R., et al 2001, *A&A*, 365, L104
- Peterson, J. R., Kahn, S., Paerels, F., Kaastra, J., Tamura, T., Bleeker, J., Ferrigo, C., & Jernigan, J. 2003, *ApJ*, 590, 207
- Pfrommer, C., & Ensslin, T. 2004, *A&A*, 413, 17
- Quataert, E. 1998, *ApJ*, 500, 978
- Quataert, E. 2005, in preparation.
- Rechester, R., & Rosenbluth, M. 1978, *Phys. Rev. Lett.*, 40, 38
- Reimer, O., Pohl, M., Sreekumar, P., & Mattox, J. 2003, *ApJ*, 588, 155
- Reynolds, C. S. 2002, in *ASP Conf. Proc.*, 250, *Particles and Fields in Radio Galaxies*, ed. R. A. Laing, & K. M. Blundell (San Francisco: ASP), 449
- Reynolds, C. S., McKernan, B., Fabian, A., Stone, J., & Vernaleo, J. 2005, *MNRAS*
- Rosner, R., & Tucker, W. 1989, *ApJ*, 338 761
- Ruszkowski, M., & Begelman, M. 2002, 581, 223
- Ruszkowski, M., Bruggen, M., & Begelman, M. 2004a, *ApJ*, 611, 158
- Ruszkowski, M., Bruggen, M., & Begelman, M. 2004b, *ApJ*, 615, 675
- Ryu, D., Kim, J., Hong, S., & Jones, T. 2003, *ApJ*, 589, 338
- Schmidt, R. W., Allen, S. W., & Fabian, A. C. 2004, *MNRAS*, 352, 1413
- Shu, F. 1974, *A&A*, 33, 55
- Suginohara, T., & Ostriker, J. 1998, *ApJ*, 507, 16
- Sun, M., Jones, C., Murray, S., Allen, S., Fabian, A., & Edge, A. 2003, *ApJ*, 587, 619
- Tabor, G., & Binney, J. 1993, *MNRAS*, 263, 323
- Tamura, T. et al 2001, *A&A*, 365, L87
- Taylor, G., Fabian, A., Allen, S. 2002, *MNRAS*, 334, 769
- Taylor, G., Govoni, F., Allen, S., Fabian, A. 2001, *MNRAS*, 326, 2

- Tornatore, L., Borgani, S., Springel, V., Matteucci, F., Menci, N., & Murante, G. 2003, MNRAS, 342, 1025
- Tozzi, P., & Norman, C. 2001, ApJ, 546, 63
- Travis, L., & Matsushima, S. 1973, ApJ, 180, 975
- Ulrich, R. 1976, ApJ, 207, 564
- Vainshtein, S., & Rosner, R. 1991, ApJ, 376, 199
- Vogt, C., & Ensslin, T. 2005, A&A, 412, 373
- Vogt, C., & Ensslin, T. 2005, astro-ph/0501211
- Voigt, L., & Fabian, A. 2004, MNRAS, 347, 1130
- Voit, G. M., Bryan, G. L., Balogh, M. L., & Bower, R. G. 2002, ApJ, 576, 601
- Wise, M. W., McNamara, B. R., & Murray, S. S. 2004, ApJ, 601, 184
- Xiong, D. R. 1991, Proc. Astr. Soc. Australia, 9, 26
- Yan, H., & Lazarian, A. 2004, ApJ, 614, 757
- Zakamska, N., & Narayan, R. 2003, ApJ, 582, 162